Safety factor measurements on the magnetic axis of the Texas experimental tokamak plasma in Ohmic and electron-cyclotron-resonance heated discharges

L. K. Huang, M. Finkenthal,* D. Wróblewski,† and H. W. Moos
The Johns Hopkins University, Baltimore, Maryland 21218

W. P. West
General Atomics, San Diego, California 92318

P. E. Phillips and D. C. Sing
The University of Texas at Austin, Austin, Texas 78712
(Received 22 May 1991)

Analysis of the circular polarization of a spectral line emission inside plasmas provides a measurement of the poloidal magnetic field on the Texas experimental tokamak (TEXT). Three sets of different polarimeters, using, respectively, the Ti XVII 3834-Å line of the intrinsic titanium impurity and the Li I 6708-Å line of a monoenergetic lithium beam, were developed and operated on TEXT. The safety factor q on the magnetic axis, determined from the measured magnetic field, was found to be near unity in all cases of Ohmically heated sawtoothing and nonsawtoothing discharges, and significantly below unity in the case of electron-cyclotron-resonance heating at the plasma center for high edge q discharges.

PACS number(s): 52.35.Py, 52.55.Fa, 52.70.Kz

I. INTRODUCTION

Measurements of the safety factor on the magnetic axis q_0 for Ohmically heated (steady) sawtoothing discharges of tokamak plasmas have been a long-standing important subject for plasma-instability studies [1]. As listed in Table I [2–13], the measurements on various tokamaks with different diagnostics claimed conflicting q_0 values, either near unity ($q_0=1.0\pm0.1$) or significantly below unity ($q_0<0.9$), which stand for either supporting or challenging the theory that the sawtoothing activity occurs when $q_0<1.0$, preventing q_0 from reaching values significantly below unity in the Ohmically heated discharges [1]. Extensive theoretical efforts have provided various physical models for the sawtoothing activities [1,14–22]. None of them gave satisfactory explanations of the experimental findings. The results of experimental studies are inconclusive. For nonsawtoothing discharges, most of the diagnostics [2,3,5,7,9,23,24], except the result on TEXTOR [4], consistently demonstrated q_0 values near or larger than unity, as shown in Table II, in agreement with the prediction for q_0 in magnetohydrodynamically (MHD) stable plasmas [1].

It has also been observed that radio-frequency wave heating and neutral-beam heating could stabilize MHD instabilities [5,25,26]. Such auxiliary heating increases the local plasma temperature, which, in turn, changes the plasma current-density distribution and modifies the q profile. When auxiliary heating takes place at the plasma center, q_0 is expected to be significantly below unity regardless of internal disruptions. Coupled with observations of sawtoothing activity associated with auxiliary heating, measurements of changes in the q profile may help in understanding the instabilities.

Most of the quoted q_0 diagnostics provided time-averaged measurements over many sawtooth periods. Both the measured electron temperature and soft-x-ray emission in the plasma center increased steadily in a large portion of a sawtooth period, then crashed rapidly to a lower level in $<10\%$ of the period [27,28]. The magnetic-flux-surface reconnection may occur during the crash according to some theories [1,14]. Nonlinear q_0 evolution in time after a sawtooth crash was suggested. Thus, the time-averaged q_0 measurements are heavily weighted towards the stable regime before the crash. There were two experimental reports which showed that measured q_0 values decreased to a lower level before a sawtooth crash and increased to a higher level after the crash [24,29]. The estimated $\Delta q_0/q_0$ values during a crash were on the order of $\simeq 10\%$. Therefore, a time-averaged q_0 value should appear near unity (1.0 ± 0.1) if the MHD activities become unstable when $q_0<1$, and it should appear significantly below unity (<0.9) if the MHD activities become unstable only when q_0 is significantly below unity. Theories to understand the different experimental findings of q_0 values require different assumptions of plasma profiles, use different scaling in approximations, and derive different instability models [1,14–22]. Thus, the time-averaged measurements, though only restricting q_0 to certain ranges rather than to a precise value, are of importance.

Exploratory work on using the circular polarization of Zeeman-split spectral line emissions to measure the poloidal magnetic field began on the Texas experimental tokamak (TEXT) in early 1986 [30]. The basic theory for this work has been described elsewhere [11,31–35]. Briefly, the amplitude of the intensity difference between left-hand and right-hand circularly polarized line profiles

(the circular polarization) is proportional to the local magnetic field component in the emission direction when the line is emitted from a localized spectral source. If an observation direction is in a tokamak poloidal plane, the poloidal magnetic field can be derived from the measured circular polarization. In developing this technique, the Ti XVII 3834-Å-line emission of intrinsic titanium impurities was chosen first, and q_0 values near unity were reported for Ohmically heated sawtoothing discharges [8,32]. Later, the Li I 6708-Å-line emission of a monoenergetic lithium beam was studied, and q_0 values similar to those obtained using the titanium line were found [11]. However, the lithium beam provided a localized spectral source, thus yielding a localized measurement. In both experiments, the polarimeters used a scanning Fabry-Pérot interferometer to scan the spectral line profiles at a rate of longer than 100 ms per order of interference maxima. These measurements were made only when the interferometer scanned through the interference maxima. In the latest experiment, we developed a new polarimeter, using interference filters with ~2-Å bandpass to measure continuously at the two extremes of the circular polarization profile [31]. All three types of polarimeters were calibrated *in situ* using the known toroidal magnetic field; each calibration was independent and consequently different from the others.

We have found repeatedly that the q_0 values for the Ohmically heated sawtoothing on TEXT were near unity. Also q_0 values significantly below unity were determined in high (edge) q_a discharges with the electron-cyclotron-resonance heating (ECRH) on the magnetic axis. The present paper summarizes the q_0 measurements with three different polarimeters on TEXT. We examine all measurements for the Ohmically heated sawtoothing and nonsawtoothing discharges. A statistical evaluation of large numbers of measurements for the Ohmic discharges is given to ascertain the accuracy of the q_0 measurements. The present paper also reports the q_0 measurements and the correlation between q_0 and sawtoothing activities in the ECRH discharges. The paper is organized as follows: Section II briefly describes the experi-

TABLE I. Experimentally estimated q_0 values for Ohmically heated sawtoothing discharges on various tokamaks.

Tokamak	State[a]	Diagnostics	Spatial resolution[b]	Flux surface[c]	q_0	Δq_0	Reference
ATC	steady	fast neutral-particle orbit	L	circular	~1.0	±0.1	[2]
Tokapole II	I_p ramp	magnetic probe	L	$q=1$ near separatrices	~0.6	±0.1	[3]
TEXTOR	steady	Faraday rotation	I	circular	~0.63	±0.1	[4]
ASDEX	steady	linear polarimetry of Li^0 emission	L	circular	>0.9		[5]
JET	steady	estimated from "snake oscillation"	L	elongated	~0.97		[6]
TEXT	steady	Li^0-laser fluorescence	S	circular	~0.7	±0.05	[7]
TEXT	steady	circular polarimetry of Ti^{+18} emission	I	circular	~1.0	±0.1	[8]
TCA	steady	Alfvén waves	L	circular	~1.0	± 0.08	[9]
PBX-M	steady	H_α motional Stark effect	L	bean-shaped	~0.86	± 0.05	[10]
TEXT	steady	circular polarimetry of Li^0 emission	L	circular	~0.94	±0.06	[11]
JET	steady	Faraday rotation	I	elongated	~0.74		[12]
DIII-D	steady	H_α motional Stark effect	L	elongated	~1.0	±0.2[d]	[13]

[a]The plasma states during the measurement: steady stands for a state when the plasma parameters remain constant; I_p ramp, for when the plasma current changes.

[b]L stands for a localized measurement; I for a deconvolution of chord integration, and S for a deconvolution of spatially smeared signals.

[c]The noncircular flux surfaces were constructed from solutions to the Grad-Shafranov equation that satisfy the boundary flux measurements and/or the profiles of the electron density, the electron temperature, and the soft-x-ray emission.

[d]The measurement was taken at 2.1-MW neutral-beam injection. When the neutral-beam heat power increased to 4.8–16.2 MW, q_0 ranged from 0.74 to 0.87 [24].

TABLE II. Experimentally estimated q_0 values for Ohmically heated nonsawtoothing discharges on various tokamaks. (A key to footnotes a,b, and c appears at the bottom of Table I.)

Tokamak	State[a]	Diagnostics	Spatial resolution[b]	Flux surface[c]	q_0	Δq_0	Reference
ATC	steady	fast neutral-particle orbit	L	circular	>1.0		[2]
Tokapole II	I_p ramp	magnetic probe	L	noncircular	>1.0	±0.1	[3]
TEXTOR	steady	Faraday rotation	I	circular	~0.78	±0.12	[4]
ASDEX	steady	linear polarimetry of Li^0 emission	L	circular	>1.0		[5]
TEXT	steady	Li^0-laser fluorescence	S	circular	~1.1	±0.1	[7]
TCA	steady	Alfvén waves	L	circular	>1.0		[9]
TFTR	I_p ramp	polarimetry of Li pellet	L	circular	~1.0		[23]
DIII-D	I_p ramp	H_α motional Stark effect	L	elongated	~1.0	±0.2	[24]

ment. Section III presents and discusses the q_0 measurements for the Ohmically heated discharges. Section IV gives the results for the ECRH discharges, followed by a brief summary. Details of the spectroscopic theory, instrumentation and data analysis methods for the diagnostics have been described in Refs. [11] and [26–30].

II. EXPERIMENT

TEXT has a 100-cm major radius and a 26-cm minor radius [36]. The toroidal magnetic field B_t is in a range of 1–3 T. The plasma current is in a range of 100–300 kA. The steady-state phase (with approximately constant values for the total plasma current, electron density, soft-x-ray emission, and toroidal magnetic field) in a 500-ms discharge is 200–300 ms. The measurements of the tangential poloidal magnetic field B_θ were made during the steady-state phase. To achieve required measurement accuracy, the data were averaged over 2–10 discharges with an $\simeq$50-ms integration time for each data point. Radial profiles of B_θ were obtained by a radial scan on a shot-by-shot basis. Each measurement was an average over several hundred sawtoothing periods since the sawtoothing period on TEXT was about 1 ms [37]. Figure 1 shows two measured B_θ, profiles, using the lithium-beam emission, before and during ECRH discharges.

Measured q_0 values for the Ohmically heated discharges and the ECRH discharges are listed in Tables III–V, respectively. The tables compile all of the measurements made by the diagnostic, including some very noisy data sets. The polarimeters, as well as the spectral lines, used in the experiment are indicated for each measurement in the tables. The three polarimeters were calibrated independently. With each polarimeter, the same calibration was used for all of its measurements.

In order to obtain q_0 various fitting procedures for the measured B_θ profiles were used. In the experiment with the lithium beam, measured B_θ radial profiles were fitted with a toroidally corrected poloidal-field B_θ function [11]. The B_θ function was constructed from a cylindrical current-density profile $j(\rho)$, which was a modified Gaussian function with adjustable parameters. The Shafranov toroidal correction does not affect the derived q_0 value, even though it significantly modifies B_θ near the plasma edge [38]. The derived q_0 is insensitive to chosen fitting functions when there are sufficient data points near the magnetic axis. Details about the B_θ fitting can be found in Ref. [11]. For measurements with the data points only inside the sawtooth inversion radius, where the current-density profile was flat as shown in Fig. 2, a straight-line fitting was used. However, this straight-line fitting overestimates q_0 by ~0.07, which was estimated by fitting a straight line to a B_θ profile inside a $q=1$ radius. To fit measurements near the plasma center for nonsawtoothing discharges, only parabolic functions was used.

With the Ti XVII 3834-Å line emission, we fit the line-integrated measurements by

$$B_c(x)=\frac{\int_{-y_0}^{y_0} dy\,\epsilon(\rho)B_\theta(\rho)\cos\theta}{\int_{-y_0}^{y_0} dy\,\epsilon(\rho)}\ , \tag{1}$$

where x is a chord position coordinate originating at the center of the outmost flux surface, $y_0=(a^2-x^2)^{1/2}$, ρ is a radius of a flux surface tangent to the line of sight, $\cos\theta$ is a cosine function of the projection angle between the tangent of a flux surface and the line of sight, ϵ is the volume emissivity, which is Abel-inverted from the line-brightness profile, and $B_\theta(\rho)$ is the toroidally corrected tangential poloidal magnetic field. Effects of the titanium-ion temperature are unimportant [8]. For the

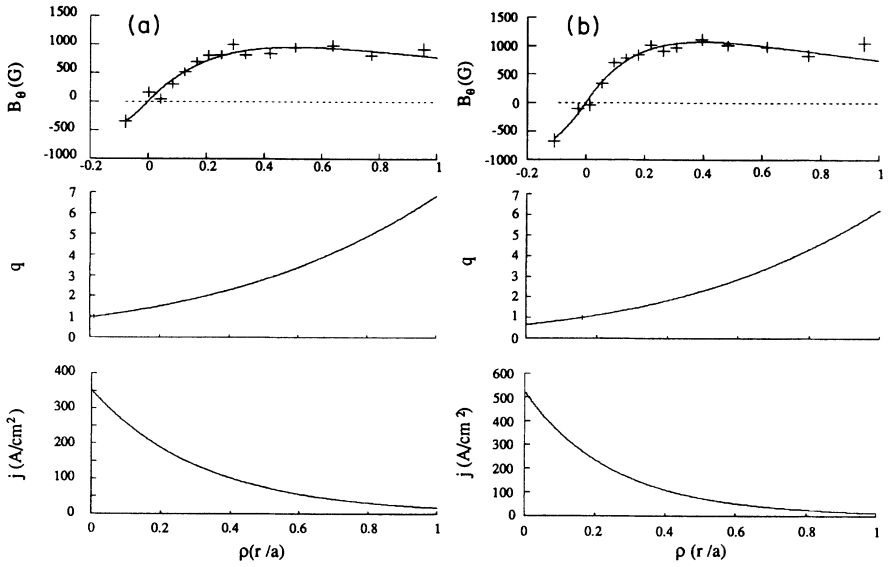

FIG. 1. The measured poloidal-magnetic-field profiles for the $q_a = 6.6$ discharges with ECRH on the magnetic axis for the focused-antenna experiment. The polarimeter continuously measured B_θ (a) before ECRH and (b) during ECRH. The Li I 6708-Å line from a lithium-beam emission was used for a localized measurement. The toroidally corrected B_θ profiles (solid lines) are used to fit the measurements. The safety factor profile q and the current-density profile j are derived from the fitting.

$q_a = 2.0$ discharges, the full widths at half maximum (FWHM) of the Ti XVII 3834-Å line profiles were $\Delta\lambda = 1.40 \pm 0.04$ Å, measured from the center to the edge of the plasma. This approximately constant FWHM indicated a flat ion-temperature profile for the titanium ions. Large instrumental broadening also made the FWHM less sensitive to the ion temperature. Thus, an estimated uncertainty due to the variation of the titanium-ion temperature along the line of sight is less than 3% (because $B_c \propto \Delta\lambda$). The line-integrated measurement is highly weighted toward the plasma center by the line emissivity profile. In order to estimate the q_0 uncertainty due to ϵ, we varied the emissivity-profile width by ±25% in the fitting. It caused a variation of ±5% in the derived q_0 for $q_a = 3.3$ discharges, and a variation of ±1% for $q_a = 2$ discharges. Both are included in the error bars. This low sensitivity to ϵ can be understood as follows. For the low-q_a discharges, the current-density profile was very flat near the plasma center, as shown in Fig. 2. $B_\theta(\rho)$ inside the sawtooth inversion radius, where the line emission was highly peaked, was approximately proportional to ρ, and $B_\theta \cos\theta$ was approximately a constant integrant to be factored out of the integration in Eq. (1), and thus the integration depended only weakly on ϵ.

TABLE III. Measured q_0 for Ohmically heated nonsawtoothing discharges on TEXT.

B_t[a]	I_p[a]	$\bar{n}_e$[a]	q_a	$q_0 \pm \Delta q_0$	Diagnostic[b]	Fit[c]
28	190	1.5	4.9	0.97±0.22	Ti	S
28	150	2.0	6.2	1.32±0.43	Li-*S*	B
21.6	115	1.5	6.3	0.97±0.08	Li-*S*	B
21.6	120	1.5	6.1	0.99±0.06	Li-*C*	P
21.6	120	1.5	6.1	1.00±0.09	Li-*C*	P
21.6	120	1.5	6.1	0.99±0.08	Li-*C*	P
19	120	1.5	5.3	0.98±0.12	Li-*C*	P
21.6	110	1.4	6.6	0.98±0.09	Li-*C*	B

[a]Discharge conditions: toroidal magnetic field B_t in kG, plasma current I_p in kA, and line-averaged electron density $\bar{n}_e$ in 10^{13} cm^{-3}. All measurements were made for the hydrogen discharges.

[b]Diagnostic: Ti stands for using the scanning polarimeter with the Ti XVII 3834-Å line, Li-*S* for using the scanning polarimeter with the Li I 6708-Å line, and Li-*C* for using the nonscanning polarimeter with the Li I 6708-Å line.

[c]Fitting procedure: B stands for the $B_\theta(\rho)$ fitting of the locally measured B_θ profile, S for a spatial inversion by the $B_c(x)$ fitting of the line-integrated profile, and P for a parabolic function fitting of the locally measured B_θ profile inside $r = 12$ cm.

TABLE IV. Measured q_0 for Ohmically heated sawtoothing discharges on TEXT. (A key to footnotes a, b, and c appears at the bottom of Table III, except that for this table L in footnote c denotes a straight-line fitting of the measurements near the magnetic axis.)

B_t[a]	I_p[a]	$\bar{n}_e$[a]	q_a	$q_0 \pm \Delta q_0$	Diagnostics[b]	Fit[c]
20	200	1.5	3.3	0.96±0.23	Ti	S
15	250	1.0	2.0	1.00±0.10	Ti	L
18	300	2.0	2.0	1.00±0.10	Ti	L
18	300	1.5	2.0	0.99±0.08	Ti	S
18	300	1.5	2.0	0.94±0.06	Li-*S*	B
19	200	1.5	3.2	1.10±0.10	Li-*S*	L
22	200	1.5	3.7	1.02±0.06	Li-*S*	L
19	200	1.6	3.2	0.91±0.47	Ti	S
24	200	1.6	4.0	1.37±0.22	Ti	S
22	200	1.8	3.7	1.12±0.52	Ti	S
22	200	2.5	3.7	1.04±0.12	Ti	S
17	120	1.5	4.8	1.19±0.17	Li-*C*	L
15	120	1.5	4.2	1.06±0.08	Li-*C*	L

In the extreme case of the $q_a = 2$ discharges in which the current-density profiles were very flat [11], the integration led to $B_c(x) \simeq B_\theta(x)$, measured on the midplane. This justifies the use of a straight-line fitting of the measured $B_c(x)$ inside the sawtooth inversion radius for the $q_a = 2$ discharges.

III. OHMICALLY HEATED DISCHARGES

A. Nonsawtoothing discharges

Table III presents eight q_0 measurements for the nonsawtoothing discharges with q_a ranging from 4.9 to 6.6. All measured q_0 values for the nonsawtoothing discharges are very close to unity, with the exception of the $q_a = 6.2$ discharge, which has a large uncertainty because of low lithium-beam penetration in a high-density plasma. A statistical average of the q_0 values weighted with the error bars is $\bar{q}_0 = 0.98 \pm 0.03$.

For the $q_a = 4.9$ discharges, a steady MHD oscillation at ~9 kHz existed in the soft-x-ray emission at $r = 1.5$ cm. The mode was identified as $m = 1$. When q_a was reduced to 4.8, the oscillation became the precursor oscillation, and grew to an internal disruption. When q_a was increased to 5.3, the oscillation disappeared. If the $m = 1$ mode is associated with the $q = 1$ resonance flux surface

TABLE V. Measured q_0 for the ECRH discharges.

B_t[a]	I_p[a]	$\bar{n}_e$[a]	ECRH[b]	$q_0 \pm \Delta q_0$	ρ_s[c]	ρ_q[d]	β_p	β'_p[e]
21.6	114	1.4	190 U	0.55±0.08	0.15 A	0.20	0.186	0.224
21.6	110	1.4	B	0.94±0.08	N	~0	0.158	
21.6	114	1.4	190 U	0.73±0.18	0.15 A	0.23	0.144	0.220
21.6	110	1.4	B	0.98±0.09	N	~0	0.196	
21.6	114	1.4	160 F	0.66±0.05	S	0.15	0.281	0.253
21.6	114	1.4	A	0.68±0.05	S	0.15	0.213	0.212
18.0	300	1.4[f]	O	0.94±0.06	0.40	0.38	0.083	0.026

[a]Discharge conditions: toroidal magnetic field B_t in kG, plasma current I_p in kA, and line-averaged electron density $\bar{n}_e$ in 10^{13} cm^{-3}. All measurements were conducted for the hydrogen-gas discharges. Three sets of data for ECRH discharges are separated by space in the table.

[b]ECRH was switched on at 300 ms and off at 375 ms. The numbers indicate the ECRH power in kW when the measurements were taken; "U" stands for using unfocused antenna; "F" stands for using focused antenna; "B" stands for the measurements taken before ECRH and "A" stands for those taken after ECRH. "O" indicates Ohmic heating only.

[c]ρ_s is the sawtooth inversion radius of the soft-x-ray emission, normalized to the minor radius. "A" indicates that ρ_s was taken after ECRH, while no sawtoothing activities were identified during ECRH. "N" indicates no sawtoothing activities were identified before ECRH. "S" indicates sawtoothing activities were observed in the soft-x-ray emission, but ρ_s measurements were not available.

[d]Radius at $q = 1$.

[e]The pressure gradient, $\beta'_p = (8\pi/B_s^2) \int_0^{\rho_q} (\rho/\rho_q)^2 (-dP/d\rho) d\rho$, where B_s is the field B_θ at the $q = 1$ surface.

[f]An Ohmically heated sawtoothing discharge with a very flat q profile inside ρ_q. It is listed in the table for comparison.

as many theories predict [1,14–22], one could conclude that the $q=1$ surface for the $q_a=4.9$ discharge was at $r=1.5$ cm. A parabolic q profile having $q=1$ and $q_a=4.9$ at the given positions gives $q_0=0.99$. The B_θ measurement showed a most probable value of $q_0=0.97$. We may also assume that q_0 for the $q_a=5.3$ discharges is just above unity since the MHD oscillation disappeared at this q_a value. The B_θ measurement showed a most probable value of $q_0=0.98$. We found that the q_0 values for the $q_a=6.6$ discharges remain very close to unity. This is in agreement with the q_0 values derived from measured electron-temperature profiles with a Spitzer resistivity, a constant Z_{eff}, and a constant loop voltage.

The present diagnostic agrees with most diagnostics on various tokamaks that the q_0 values for the Ohmically heated nonsawtoothing discharges are near or larger than unity [2,3,5,7,9,23,24], and disagrees with the result on TEXTOR [4]. A statistical analysis of these results must preclude both systematic errors (such as whether all q_0 diagnostics were biased by the theoretical predictions of either $q_0 \geq 1$ or $q_0 \ll 1$ for the stable discharges) and accidental errors (such as technical problems in a diagnostic). Such a review of different diagnostics is beyond the scope of this paper.

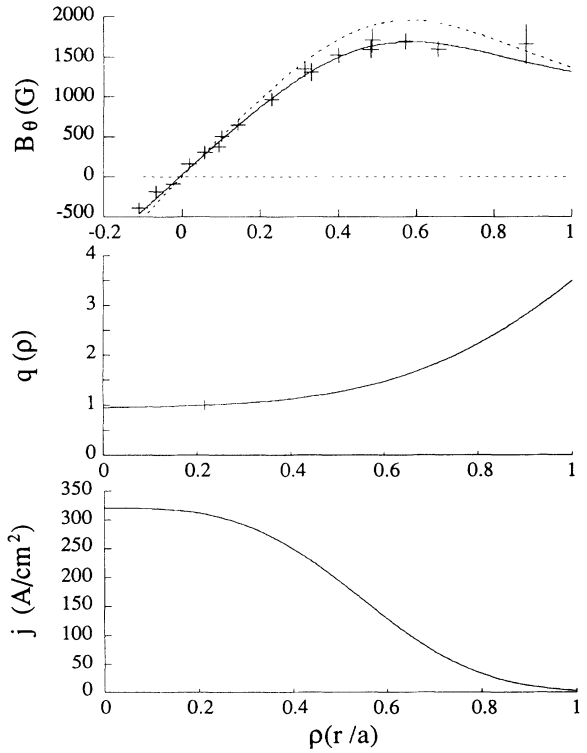

FIG. 2. A chord-averaged vertical magnetic field profile $B_c(x)$ measured with the Ti XVII 3834-Å line. The measurement is for the $q_a=3.3$ discharges listed in Table IV. The $B_c(x)$ profile (solid curve) is an integration of the vertical projection of the toroidally corrected tangential poloidal magnetic field B_θ (dashed curve). $B_c(x)$ is used to fit the measurements. Derived from the fitting, the q and j profiles show flat features inside the $q=1$ surface.

B. Sawtoothing discharges

Measured q_0 values for the Ohmically heated sawtoothing discharges are listed in Table IV. The first four measurements with the titanium line in Table IV have been published in Ref. [8]; here, the q_0 values in the first and the fourth measurements are derived by the fitting procedure which included the toroidal correction, and are in agreement with the results in Ref. [8]. All nine measurements using the titanium line, including one with nonsawtoothing discharges, have the same calibration. Three other sawtoothing discharge results, obtained using the lithium-beam emission and the scanning polarimeter and published in Ref. [11], are based on a unique calibration as for the nonsawtoothing discharges. All other measurements, obtained using the lithium-beam emission and the nonscanning polarimeter [31], also used the same calibration as for their counterparts in the nonsawtoothing discharges.

None of the discharges listed in the table have a measured q_0 value below 0.9. In order to draw a statistical conclusion from the repeated findings of $q_0>0.9$, we must preclude any systematic deviations from the measurement. The straight-line fitting in six cases in Table IV may overestimate q_0 by ~ 0.07 as discussed in Sec. II. No systematic errors other than the straight-line fitting were evident. Knowing the systematic error, we will subtract the overestimated amount from the q_0 values obtained with the straight-line-fitting procedure in the statistical analysis. Thus, these measured q_0 values are consistent with the observations using the other fitting procedures.

If the measured q_0 values in Table IV had been for the same discharge condition, we could find a most probable q_0 value by

$$\bar{q}_0=\frac{\sum_{i=1}^{n} q_{0i}\Delta q_{0i}^{-2}}{\sum_{i=1}^{n}\Delta q_{0i}^{-2}}, \tag{2}$$

and estimate the uncertainty by

$$\Delta\bar{q}_0=1/\left[\sum_{i=1}^{n}\Delta q_{0i}^{-2}\right]^{1/2}, \tag{3}$$

where q_{0i} and Δq_{0i} are the measured q_0 values and their uncertainties, and the summation is over all n measurements [39]. If the accuracy of Δq_{0i} for each measurement is the same Δq_0, then making n measurements will reduce the uncertainty to $\Delta q_0/\sqrt{n}$. In general, the q_0 values do not have to be the same for the different discharge conditions. $\bar{q}_0$ represents the most probable average of the q_0 values to be found for the Ohmically heated sawtoothing discharges, and $\Delta\bar{q}_0$ represents an average deviation in $\bar{q}_0$. Using Eqs. (2) and (3), we found $\bar{q}_0\sim 0.98$ and $\Delta\bar{q}_0\simeq 0.028$. If the q_0 values follow a normal distribution (the central-limit theory) [40], the probability for $q_0>0.9$ is 99%. However, it is difficult to determine the probability distribution for the average because of the limited number of measurements [40]. To avoid this problem and to get estimated limit, we used Chebyshev's inequality

$$P(|X-\mu| > |t|) \leq \frac{\sigma^2}{t^2} , \quad (4)$$

which states that for a random variable X with mean μ and variance σ^2, the probability of X deviating from μ by $> |t|$ is less than σ^2/t^2 [40]. The inequality is independent of the probability distribution. We found a probability larger than 87% for q_0 to be larger than 0.9 in the Ohmically heated sawtoothing discharges.

In the discussion for the nonsawtoothing discharges, the experimental observations showed evidence that the q_0 values for the nonsawtoothing discharges are near unity, and the results using the polarimeters are in agreement with the observations. Thus, the calibrations are unlikely to give overestimated q_0 values. In the case of the sawtoothing discharges, we can also argue that the q_0 values for the sawtoothing discharges are unlikely to be significantly larger than unity. Thus, the calibration is unlikely to lead to underestimated q_0 values. Therefore, the systematic errors (other than the straight-line-fitting procedure which has been accounted for) are negligible.

IV. HIGH-q_a DISCHARGES WITH ECRH AT THE MAGNETIC AXIS

The magnetic field measurements for the high-q_a discharges with ECRH on the magnetic axis were localized by using the lithium-beam line emission. The plasma conditions and the measured q_0 values are listed in Table V. The ECRH was launched into the plasma during the steady-state phase (from 300 to 375 ms). Two types of antennae were used in the ECHR experiments: an unfocused antenna was used in the earlier work, and a focused antenna, which concentrated the power on the axis appreciably better than the unfocused, was used later on [41]. The pressure gradient during ECRH in the focused-antenna experiment was higher than in the unfocused-antenna experiment, as listed in Table V. In both cases, the discharges without ECRH had no sawtoothing activities. During ECRH, the electron temperature T_e in the central plasma increased to ~ 1.4 keV from ~ 0.7 keV. The temperature reached its peak within ~ 10 ms after ECRH was turned on, and dropped back to the prior level in ~ 10 ms after ECRH was turned off. In the unfocused-antenna experiments, no sawtoothing activities could be identified in the soft--x-ray signal during ECRH; however, sawtoothing activities occurred after ECRH, and lasted about 40 ms. In the focused-antenna experiment, sawtoothing activities clearly developed in the soft-x-ray emission from the plasma center at ~ 45 ms after ECRH was turned on, and lasted about 40 ms after ECRH was turned off. The use of different antennae may be responsible for the difference in the sawtooth activities in the two experiments.

Table V lists three sets of measured q_0 values during ECRH, of which two sets are accompanied by the measurements before and after ECRH for comparison. Figure 1 shows the measured B_θ profiles before and during ECRH. Before ECRH, the measured q_0 values are near unity. All q_0 measurements during ECRH show consistently that q_0 values are driven significantly below unity by ECRH. Figure 3 illustrates how q_0 evolved in the ECRH discharges. Each set of q_0 values was obtained using the same polarimeter, alignment, calibration, and fitting procedures, thus minimizing systematic errors in the measured q_0 variations. The significant decrease of q_0 during ECRH also clearly proves the diagnostic is sensitive to the current density on the magnetic axis.

The time history of q_0 indicates that it took about 25–75 ms for the plasma current to reach a new distribution for ECRH. (The ± 25-ms uncertainty was due to the integration of the signal for 50 ms necessary for measurement accuracy.) The time scale for the change was consistent with the skin time of plasma current on TEXT [42]. After ECRH, the measured q_0 increased. There was no measurement after the lithium beam was turned off at 450 ms. The measured $q=1$ position was consistent with the soft-x-ray sawtooth inversion radius when the sawtoothing activity occurred. It is of interest to point out the following facts.

(1) There is a delay for the sawtoothing to occur after q_0 is driven below unity. In the focused-antenna experiment shown in Fig. 3, q_0 dropped within ~ 25 ms to ~ 0.75, significantly below unity. The time delay was longer than 20 ms. The current density reached a new balance in ~ 50 ms, at which point the sawtoothing activities started.

(2) Within a 10% uncertainty, the electron temperature decreased to the level before ECRH in about 10 ms after ECRH was switched off. The electron density and the

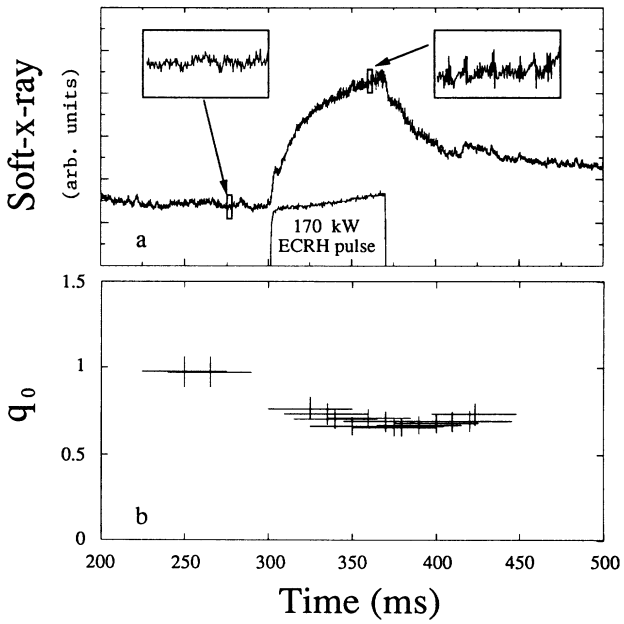

FIG. 3. The time history of q_0 measured for the ECRH discharges with the same conditions as in Fig. 1. (a) The ECRH pulse was switched on at 300 ms and off at 375 ms. The sawtoothing activities in the soft-x-ray emission occurred during and after the ECRH pulse. (b) The time history of q_0. The error bar in time was the integration time of 50 ms for sufficient accuracy in q_0. The lithium beam was turned off at 450 ms. The q_0 value rapidly decreased when ECRH was turned on, and clearly increased after ECRH. The averaging of the signals over 50 ms made the increase less visible.

ion temperature remained almost unchanged ($<10\%$) during these discharges. The pressure profile after ECRH was about the same as before the ECRH. Therefore, the sawtoothing activities after the ECRH were only related to the highly peaked current-density profile.

(3) Associated with the sawtoothing activity, the q profiles were very steep inside the $q=1$ surface since $\Delta q \simeq 0.3$ within $\Delta\rho \simeq 0.15$ (a shear of ~ 2). Such a sharp q profile with the ECRH discharges contrasts with a very flat q profile inside the $q=1$ surface for the Ohmically heated sawtoothing discharges. Their pressure gradients are listed in Table V.

V. SUMMARY

From the internal consistency of our results and the comparison with most of the available data, we conclude that the analysis of the circular polarization of the Zeeman-split spectral line emissions provides reliable q_0 measurements in a tokamak plasma. The average of measured q_0 values in the Ohmically heated nonsawtoothing discharges with q_a ranging from 4.9 to 6.6 is 0.98 ± 0.03. For all Ohmically heated sawtoothing discharges with q_a ranging from 2.0 to 4.8, the average q_0 is 0.98 ± 0.03. A statistical analysis of the results shows that the probability for $q_0 > 0.9$ is larger than 88%. The current-density profile inside $q=1$ surface is very flat for the $q_a=2$ discharge. q_0 can be driven significantly below unity (<0.73) by electron-cyclotron-resonance heating at the magnetic axis for high edge q discharges ($q_a \simeq 6$). With such a low q_0 and a large shear (~ 2) for the q profile inside the $q=1$ surface, sawtoothing activities may occur, though delayed when the current density is undergoing a redistribution. The sawtoothing activities are correlated with the very low q_0 values rather than the highly peaked plasma pressure profiles during the ECRH.

ACKNOWLEDGMENTS

The authors wish to thank Dr. M. E. Austin, Dr. Roger D. Bengtson, Dr. J. A. Boedo, Dr. R. V. Bravenec, Dr. J. Y. Chen, Dr. G. Cima, Dr. P. Edmonds, Dr. K. W. Gentle, Dr. S. C. McCool, Dr. B. U. Richards, Dr. W. L. Rowan, Dr. B. Smith, Dr. D. M. Thomas, Dr. M. P. Thomas, Dr. K. W. Wenzel, Dr. A. J. Wootton, Dr. X. Z. Yang, and Dr. Y. Z. Zhang, for discussions and collaborations when this experiment was performed. L. K. Huang is grateful to Dr. A. J. Wootton, and Dr. W. L. Rowan for their generous support during the period 1988–90. This work was supported by the U. S. Department of Energy under Grant No. DE-FG02-86ER-53214.

*Permanent address: Racah Institute of Physics, The Hebrew University, Jerusalem, Israel.

†Permanent address: Lawrence Livermore National Laboratory, University of California, Livermore, CA 94550.

[1] M. N. Rosenbluth and P. H. Rutherford, in *Fusion,* edited by E. Teller (Academic, New York, 1981), Vol. 1A, p. 31.

[2] R. J. Goldston, Phys. Fluids **21**, 2346 (1978).

[3] T. H. Osborne, R. N. Dexter, and S. C. Prager, Phys. Rev. Lett. **49**, 734 (1982).

[4] H. Soltwisch, W. Stodiek, J. Manickam, and J. Schlueter, in *Plasma Physics and Controlled Nuclear Fusion Research,* Proceedings of the Eleventh International Conference (Kyoto, 1986) (IAEA, Vienna, 1987), Vol. 1, p. 263.

[5] K. McCormick, F. X. Söldner, D. Eckhartt, F. Leuterer, H. Murmann, H. Derfler, A. Eberhagen, O. Gehre, J. Gernhardt, G. v. Gierke, O. Gruber, M. Keilhacker, O. Klüber, K. Lackner, D. Meisel, V. Mertens, H. Röhr, K.-H. Schmitter, K.-H. Steuer, and F. Wagner, Phys. Rev. Lett. **58**, 491 (1987).

[6] A. Weller, A. D. Cheetham, A. W. Edwards, R. D. Gill, A. Gondhalekar, R. S. Granetz, J. Snipes, and J. A. Wesson, Phys. Rev. Lett. **59**, 2303 (1987).

[7] W. P. West, D. M. Thomas, J. S. deGrassie, and S. B. Zheng, Phys. Rev. Lett. **58**, 2758 (1987).

[8] D. Wróblewski, L. K. Huang, H. W. Moos, and P. E. Phillips, Phys. Rev. Lett. **61**, 1724 (1988).

[9] H. Weisen, G. Borg, B. Joye, A. J. Knight, and J. B. Lister, Phys. Rev. Lett. **62**, 434 (1989).

[10] F. M. Levinton, R. J. Fonck, G. M. Gammel, R. Kaita, H. W. Kugel, E. T. Powell, and D. W. Roberts, Phys. Rev. Lett. **63**, 2060 (1989).

[11] L. K. Huang, M. Finkenthal, D. Wróblewski, H. W. Moos, W. P. West, D. M. Thomas, M. P. Thomas, X. Z. Yang, P. E. Phillips, A. J. Wootton, Roger D. Bengston, J. A. Boedo, R. V. Bravenec, J. Y. Chen, G. Cima, K. W. Gentle, S. C. McCool, B. U. Richards, W. L. Rowan, and D. C. Sing, Phys. Fluids B **2**, 809 (1990).

[12] J. Blum, E. Lazzaro, J. O'Rourke, B. Keegan, and Y. Stephan, Nucl. Fusion **30**, 1475 (1990).

[13] D. Wróblewski, K. H. Burrell, L. L. Lao, P. Politzer, and W. P. West, Rev. Sci. Instrum. **61**, 3552 (1990).

[14] B. B. Kadomtsev, Fiz. Plazmy **1**, 710 (1975) [Sov. J. Plasma Phys. **1**, 389 (1975)].

[15] M. N. Bussac, R. Pellat, D. Edery, and J. L. Soule, Phys. Rev. Lett. **35**, 1638 (1975).

[16] J. A. Wesson, Plasma Phys. Controlled Fusion **28**, 243 (1986).

[17] R. G. Kleva, J. F. Drake, and R. E. Denton, Phys. Fluids, **30**, 2119 (1987).

[18] W. Park, D. A. Monticello, and T. K. Chu, Phys. Fluids **30**, 285 (1987).

[19] A. Y. Aydemir, Phys. Rev. Lett. **59**, 649 (1987).

[20] H. L. Berk, S. M. Mahajan, and Y. Z. Zhang, Phys. Fluids B **3**, 351 (1990).

[21] J. A. Wesson, Nucl. Fusion **30**, 2545 (1990).

[22] F. Porcelli, Phys. Rev. Lett. **66**, 425 (1991).

[23] J. L. Terry, E. S. Marmar, R. B. Howell, M. Bell, A. Cavallo, E. Fredrickson, A. Ramsey, G. L. Schmidt, B. Stratton, G. Taylor, and M. E. Mauel, Rev. Sci. Instrum. **61**, 2908 (1990).

[24] D. Wroblewski, G. D. Porter, W. Meyer, L. L. Lao, R. T. Snider, W. P. West, and K. H. Burrell, Bull. Am. Phys. Soc. **35**, 1978 (1990).

[25] D. J. Campbell, J. G. Cordey, A. W. Edwards, R. D. Gill, E. Lazzaro, G. Magyar, A. L. McCrthy, J. O'Rourke, F. Pegoraro, F. Porcelli, P. Smeulders, D. F. H. Start, P. Stubberfield, J. A. Wesson, E. Westerhof, and D. Zasche,

Plasma Physics and Controlled Nuclear Fusion Research (IAEA, Vienna, 1988), Vol. I, p. 377.

[26] R. T. Snider, D. Content, R. James, John Lohr, M. A. Mahdavi, R. Prater and B. Stallard, Phys. Fluids B **1**, 404 (1989).

[27] S. V. Goeler, W. Stodiek, and N. Sauthoff, Phys. Rev. Lett. **33**, 1201 (1974).

[28] D. J. Campbell, D. F. H. Start, J. A. Wesson, D. V. Bartlett, V. P. Bhatnagar, M. Bures, J. G. Cordey, G. A. Cottrell, P. A. Dupperex, A. W. Edwards, C. D. Challis, C. Gormezano, C. W. Gowers, R. S. Granetz, J. H. Hamnen, T. Hellsten, J. Jacquinot, E. Lazzaro, P. J. Lomas, N. Lopes Cardoza, P. Mantica, J. A. Snipes, D. Stork, P. E. Stott, P. R. Thomas, E. Thompson, K. Thomsen, and G. Tonetti, Phys. Rev. Lett. **60**, 2148 (1988).

[29] H. Soltwisch, Rev. Sci. Instrum. **59**, 1599 (1988).

[30] D. Wróblewski, H. W. Moos, and W. L. Rowan, Appl. Phys. Lett. **48**, 21 (1986).

[31] L. K. Huang, M. Finkenthal, and H. W. Moos, Rev. Sci. Instrum. **62**, 1142 (1991).

[32] D. Wróblewski, L. K. Huang, and H. W. Moos, Rev. Sci. Instrum. **59**, 2341 (1988).

[33] U. Feldman, J. F. Seely, N. R. Sheely, Jr., S. Suckewer, and A. M. Title, J. Appl. Phys. **56**, 2512 (1984).

[34] V. L. Jacobs and J. F. Sheely, Phys. Rev. A **36**, 3267 (1987).

[35] R. D. Cowan, *The Theory of Atomic Structure and Spectra* (University of California Press, Berkeley, 1981).

[36] K. W. Gentle, Nucl. Technol. Fusion **1**, 479 (1981).

[37] J. A. Snipes and K. W. Gentle, Nucl. Fusion **26**, 1507 (1986).

[38] V. D. Shafranov, in *Review of Plasma Physics,* edited by A. M. A. Leontovich (Consultants Bureau, New York, 1966), Vol. 2, p. 103.

[39] P. R. Bevington, *Data Reduction and Error Analysis for the Physical Sciences* (McGraw-Hill, New York 1969).

[40] J. A. Rice, *Mathematical Statistics and Data Analysis* (Wadsworth and Brooks/Cole Advanced Books and Software, Pacific Grove, CA, 1988).

[41] D. C. Sing, V. Krivenski, M. E. Austin, J. A. Boedo, D. L. Brower, J. Y. Chen, G. Cima, K. W. Gentle, R. L. Hickok, H. Lin, N. C. Luhmann, W. A. Peebles, P. E. Philips, B. Richards, W. L. Rowan, P. M. Schoch, A. J. Wootton, X. Z. Yang, C. X. Yu, and Z. M. Zhang, *Proceedings of the Thirteenth International Conference in Plasma Physics and Controlled Nuclear Fusion Research (Washington, DC, 1990)* (IAEA, Vienna, 1991), Vol. 1, p. 757.

[42] J. L. Porter, P. E. Phillips, S. C. McCool, S. B. Kim, D. W. Ross, W. H. Miner, and J. C. Wiley, Nucl. Fusion **27**, 205 (1987).